Electronic Supplementary Material (ESI) for RSC Advances.

Electronic Supporting Information

for

Optically active blue-emitting carbon dots to specifically target the Golgi apparatus

Mengke Yuan, Yanjia Guo, Jianjia Wei, Jizhou Li, Tengfei Long, Zhongde Liu*

Key Laboratory of Luminescent and Real-Time Analytical Chemistry (Southwest University), Ministry of Education, College of Pharmaceutical Science, Southwest University, Chongqing 400716, China. Tel: +86-23-68251910. Fax: +86-23-68251048. E-mail: lzdzhy@swu.edu.cn.

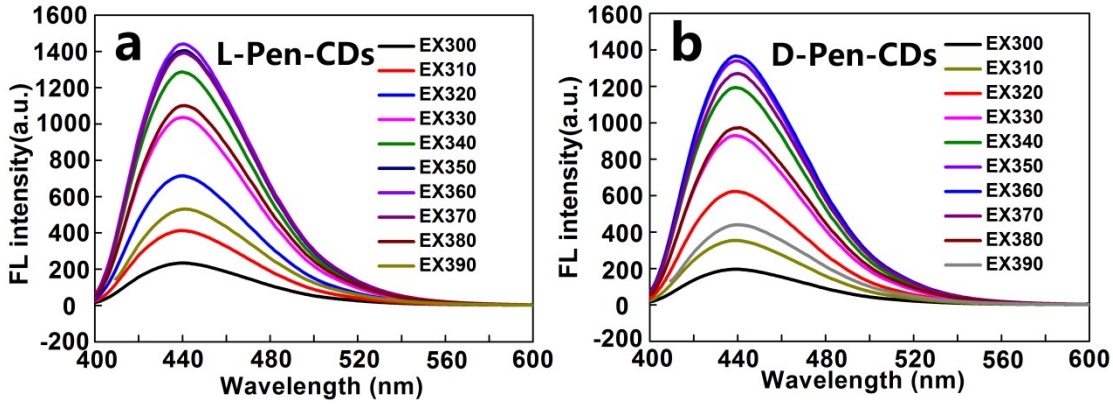

Fig. S1 The PL spectra of L-Pen CDs (a) and D-Pen CDs (b) when the excitation wavelength is changed from 300 to 390 nm.

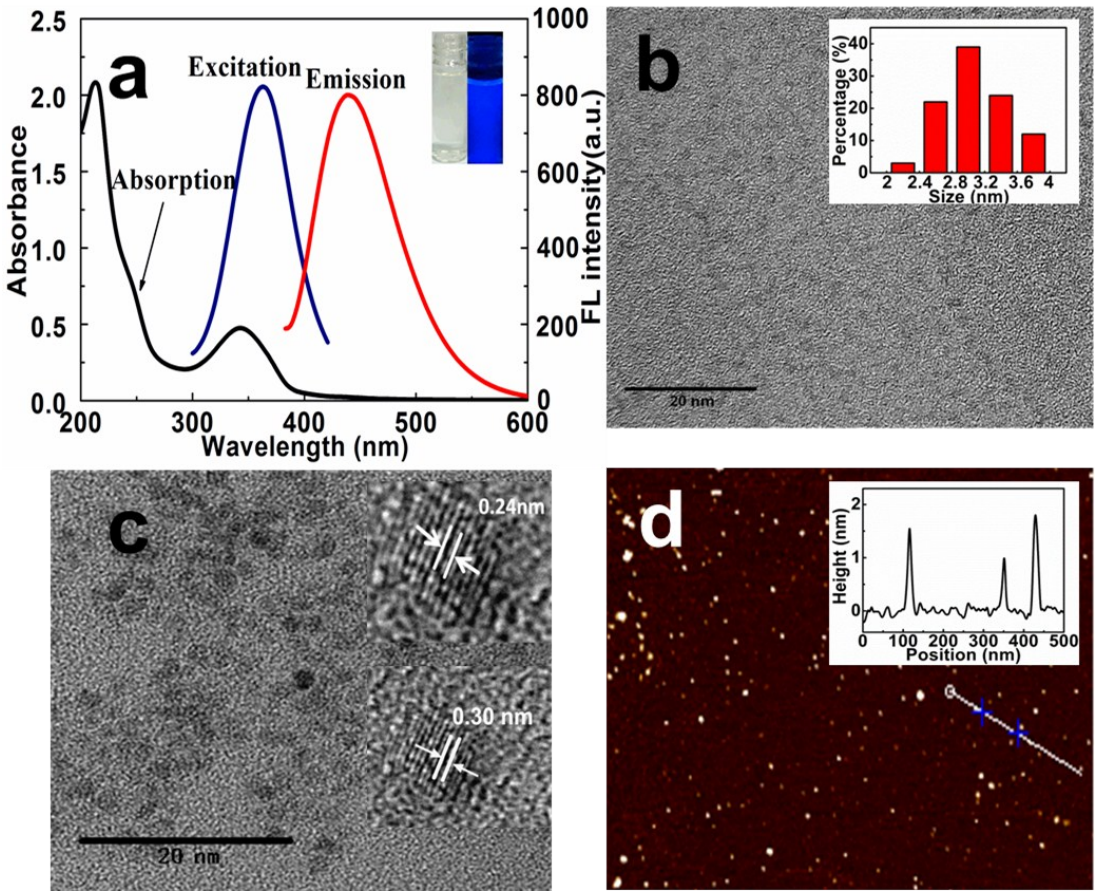

Fig.S2 Characterization of the as-prepared *D*-Pen-CDs. (a) absorption and PL spectra of *D*-Pen-CDs, the inset showing photographs of *D*-Pen-CDs under daylight and 365 nm UV light; (b, c) TEM images of the *D*-Pen-CDs, the insets are size distribution and representative lattice fringes, respectively; (d) AFM image *D*-Pen-CDs, the inset showing the section analysis along the scored line.

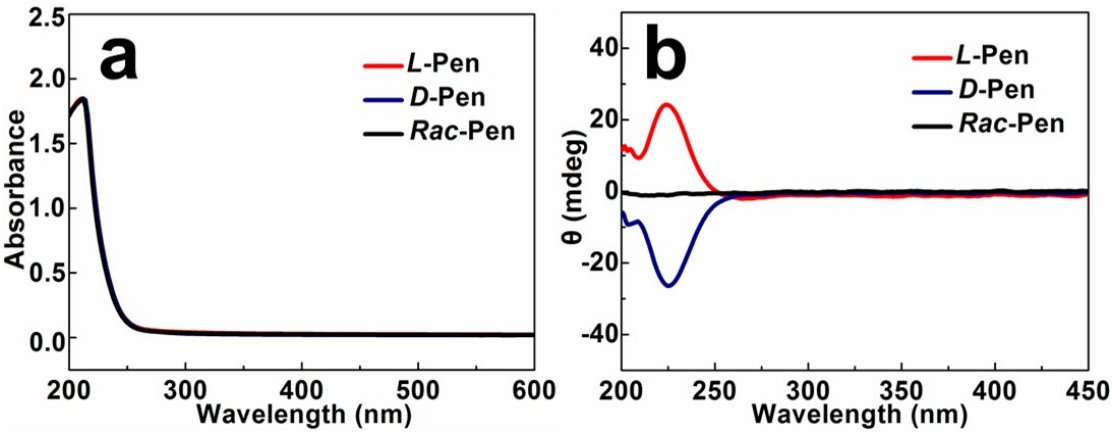

Fig.S3 UV-Vis absorption and CD spectra of pure *L*-Pen, *D*-Pen, *Rac*-Pen.

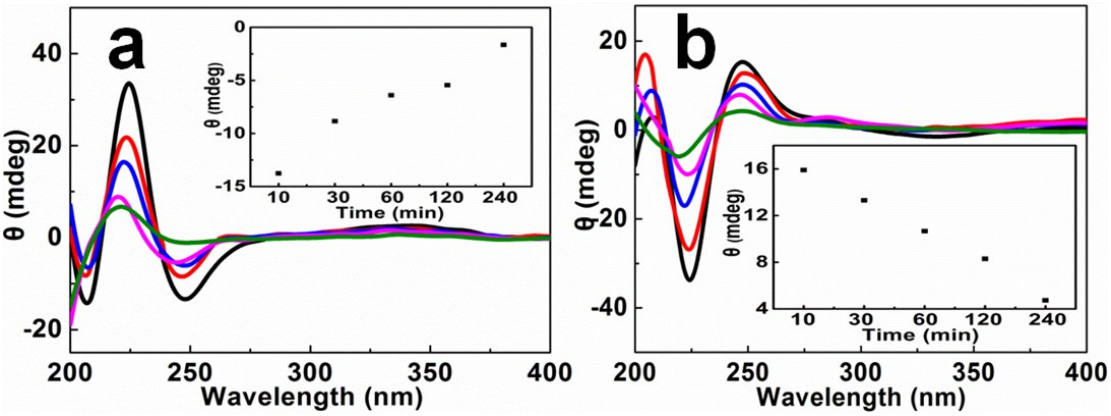

Fig.S4 Influence of the second pyrolytic reaction time on the optically active CDs. The CD spectra of *L*-Pen-CDs (a) and *D*-Pen-CDs (b) at different reaction time (black line, 10 min; red line, 30 min; blue line, 1h; pink line, 2h; green line, 4h). The insets show that the CD signals of both L-Pen-CDs and D-Pen-CDs at 247 nm gradually decrease with prolonging the time of reaction, respectively.

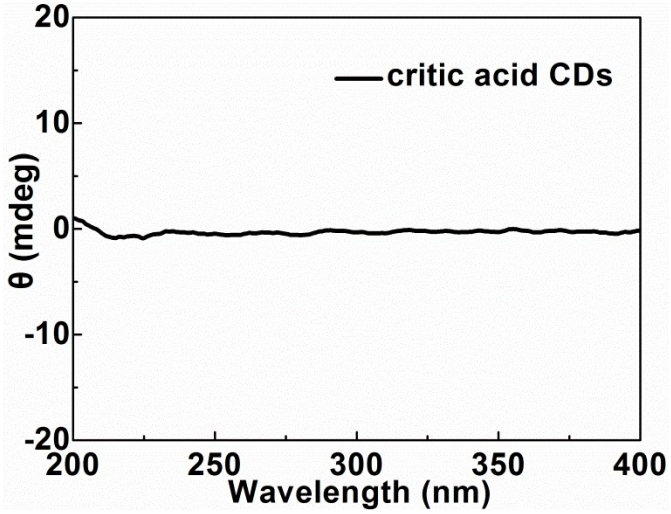

Fig.S5 The CD spectra of the pure critic acids CDs.

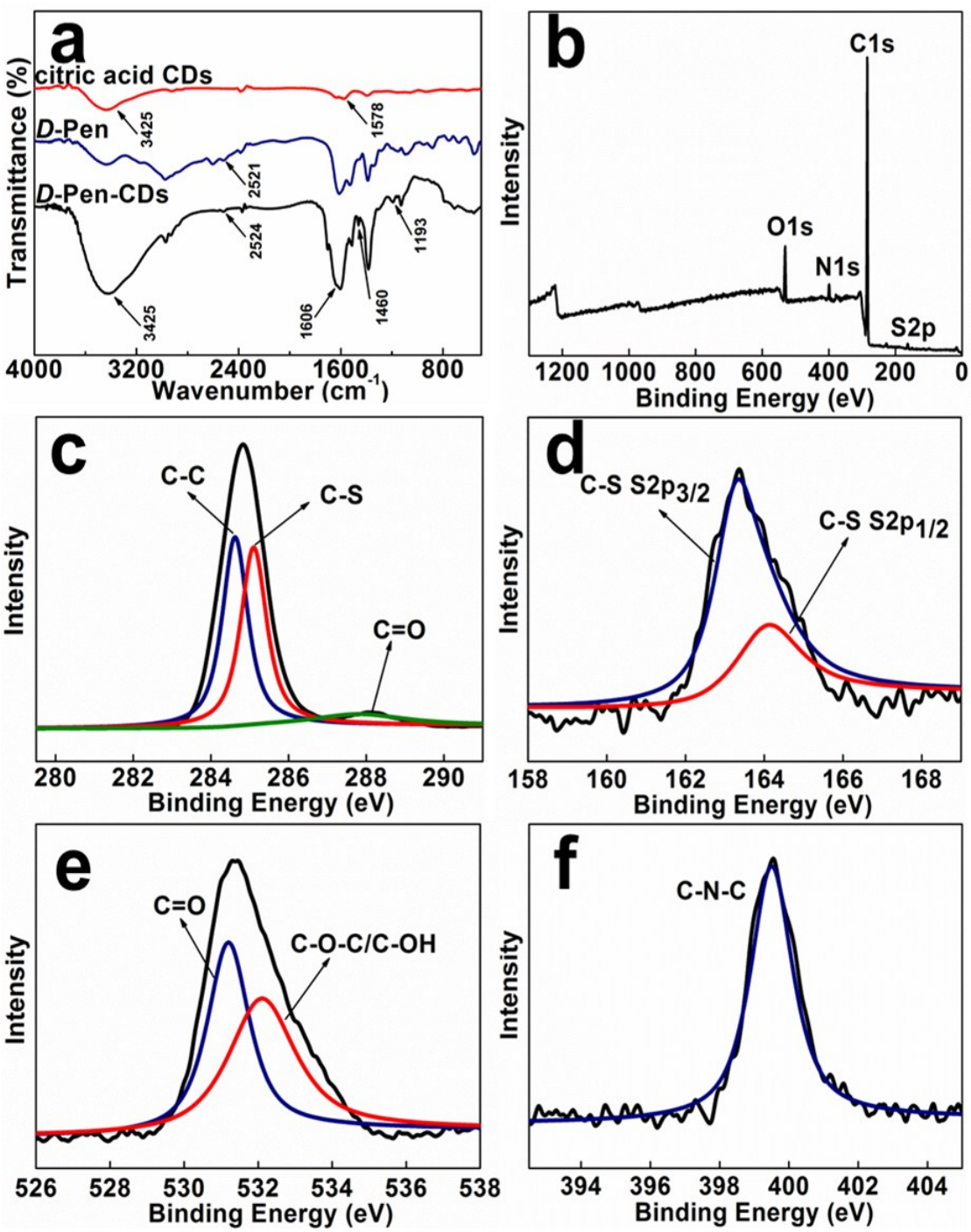

Fig.S6 FT-IR spectra of the critic acid CDs, the D-Pen alone and the D-Pen-CDs (a); XPS survey scan of the D-Pen-CDs (b); High resolution XPS spectrum of C 1s (c), S 2p (d), O 1s (e), and N 1s (f) for the D-Pen-CDs.

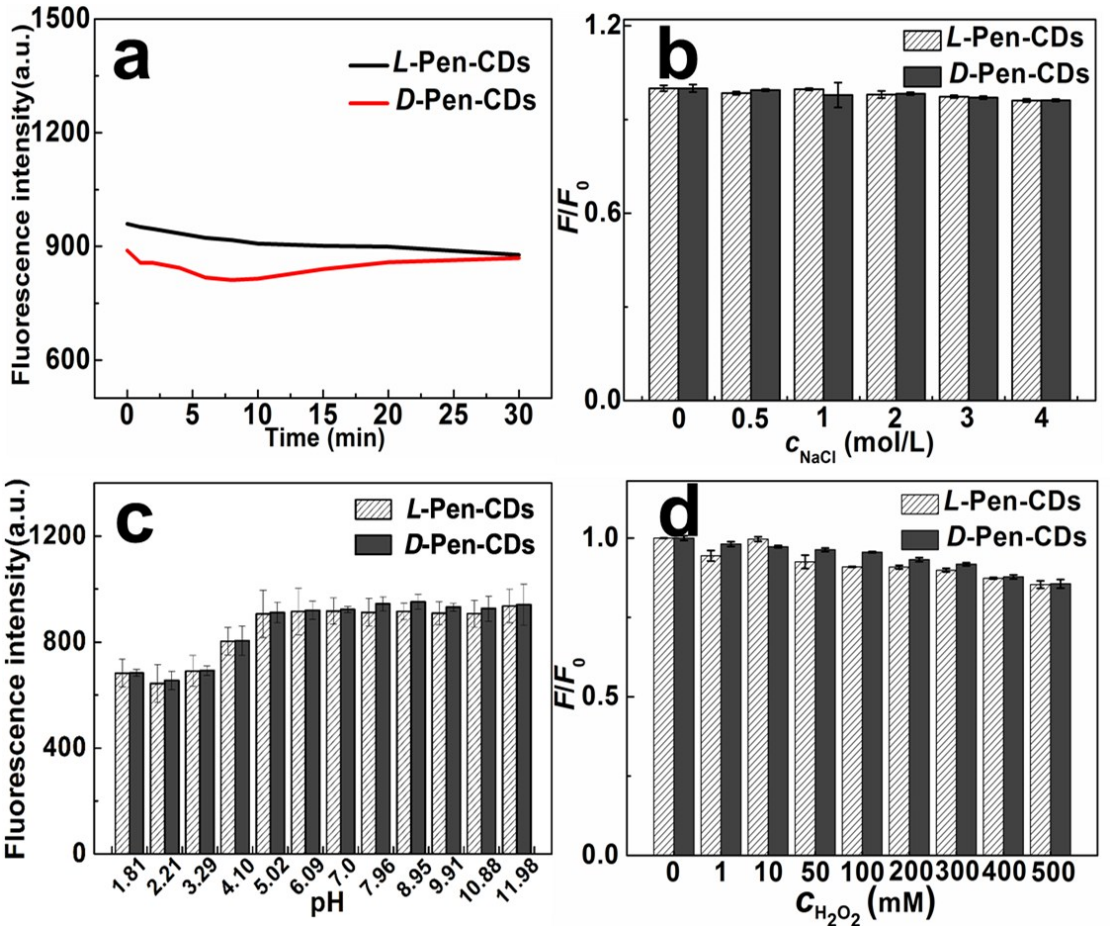

Fig.S7 Photostability of the *L*-Pen-CDs and the *D*-Pen-CDs under different illumination time (a); The salt-stability of the *L*-Pen-CDs and the *D*-Pen-CDs under different salt concentrations (b); The fluorescence intensity of the *L*-Pen-CDs and the *D*-Pen-CDs under different pH value (c); The fluorescence intensity of the *L*-Pen-CDs and the *D*-Pen-CDs under different H_2O_2 concentration (d).

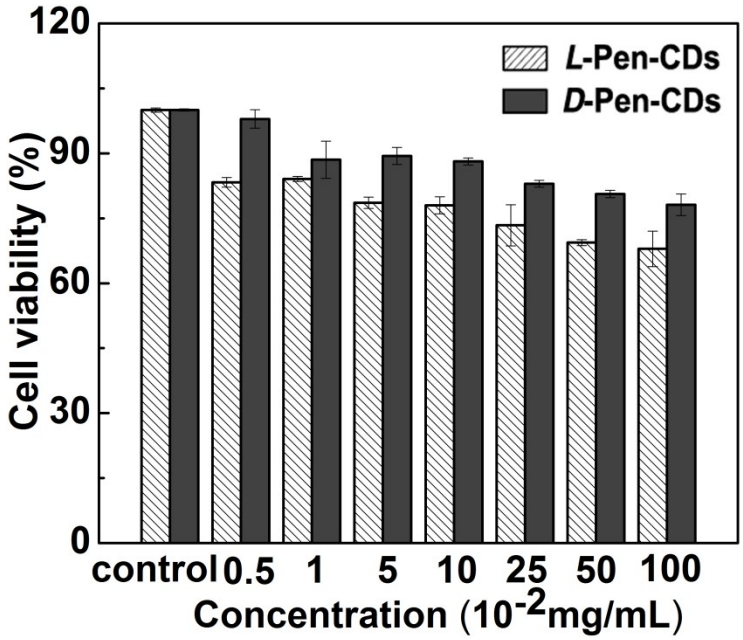

Fig.S8 Hep-2 cell growth inhibition assays of the *L*-Pen-CDs and the *D*-Pen-CDs. The cells were treated for 24 h with the *L*-Pen-CDs and the *D*-Pen-CDs at the different concentrations, respectively. All data are collected from three measurements, and the error bars indicate the standard deviation.

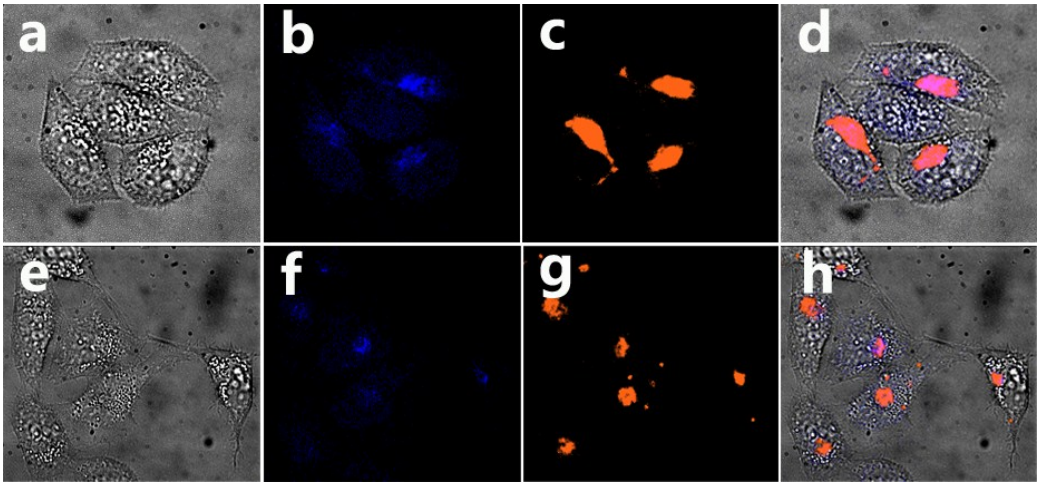

Fig.S9 The competitive inhibition of targeting ability of L-Pen-CDs (a-d) and D-Pen-CDs (e-h). The cells were incubated with L-Pen or D-Pen (0.8 mM) before the addition of L-Pen-CDs or D-Pen-CDs. Fluorescence images of L-Pen + L-Pen-CDs (b) and D-Pen + D-Pen-CDs (f). Fluorescence images of Golgi Tracker Red (c, g). Merged fluorescence and bright field images of L-Pen + L-Pen-CDs (d) and D-Pen + D-Pen-CDs (h).

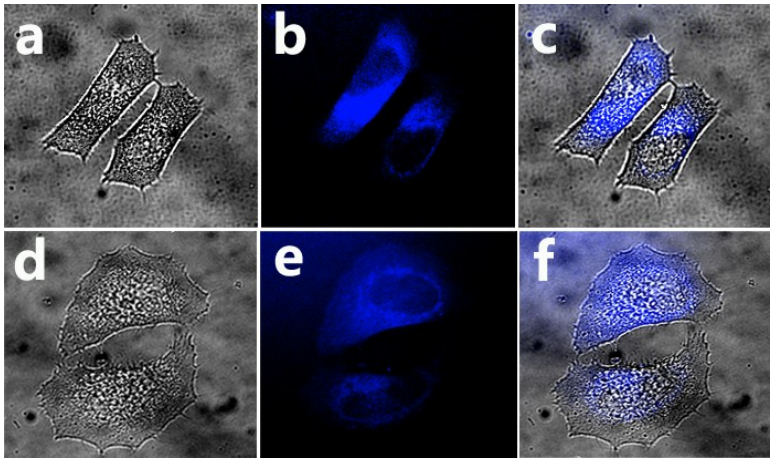

Fig.S10 Confocal microscopy images of Hep-2 cells treated with the L-alanine CDs (a-c) and D-alanine CDs (d-f), respectively. Left, Differential interference contrast (DIC) images (a, d); middle, PL images (b, e); right, merged images (c, f).

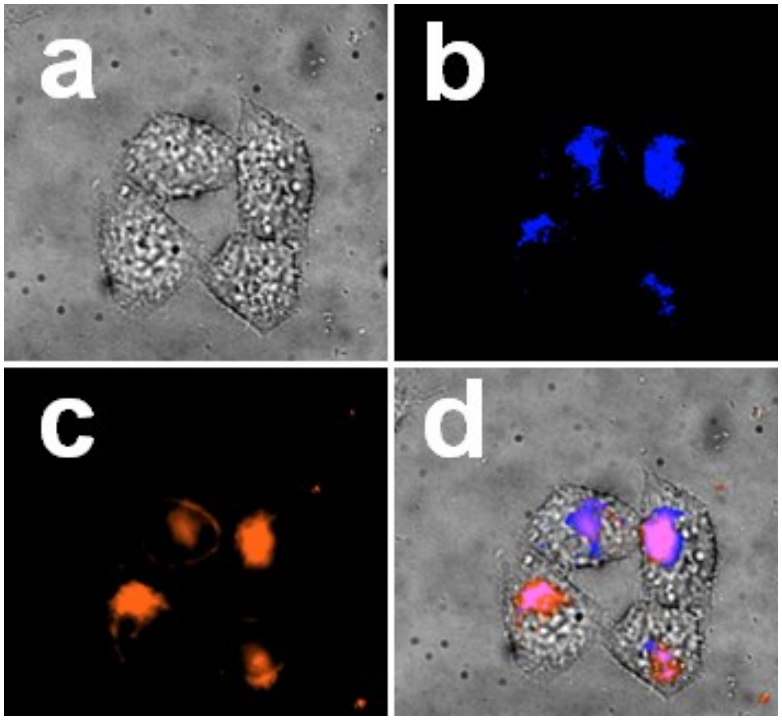

Fig.S11 Confocal microscopy images of Hep-2 cells treated with the *L*-Pen-CDs and the Golgi-Tracker Red. (a) bright field images; (b) DAPI channel; (c) CY3 channel; (d) merged fluorescence and bright field images.

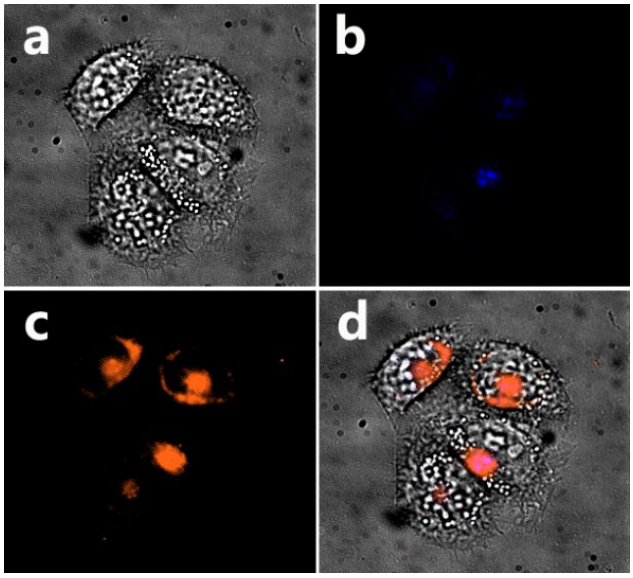

Fig.S12 Confocal microscopy images of Hep-2 cells treated with the Rac-Pen-CDs and the Golgi-Tracker Red. (a) bright field images; (b) DAPI channel; (c) CY3 channel; (d) merged fluorescence and bright field images.